ASME Letters in Dynamic Systems and Control
Online journal at:
https://asmedigitalcollection.asme.org/lettersdynsys

Improving the Performance of a Hierarchical Traffic Flow Control Framework Using Lyapunov-Based Switched Newton Extremum Seeking[1]

Pouria Karimi Shahri[2]
Department of Mechanical Engineering,
The University of North Carolina at Charlotte,
Charlotte, NC 28223
e-mail: pkarimis@uncc.edu

Baisravan HomChaudhuri
Department of Mechanical Engineering,
Illinois Institute of Technology,
Chicago, IL 60616
e-mail: bhomchaudhuri@iit.edu

Azad Ghaffari
Department of Mechanical Engineering,
Wayne State University,
Detroit, MI 48202
e-mail: aghaffari@wayne.edu

Amir H. Ghasemi
Department of Mechanical Engineering,
The University of North Carolina at Charlotte,
Charlotte, NC 28223
e-mail: ah.ghasemi@uncc.edu

The primary aim of this research paper is to enhance the effectiveness of a two-level infrastructure-based control framework utilized for traffic management in expansive networks. The lower-level controller adjusts vehicle velocities to achieve the desired density determined by the upper-level controller. The upper-level controller employs a novel Lyapunov-based switched Newton extremum seeking control approach to ascertain the optimal vehicle density in congested cells where downstream bottlenecks are unknown, even in the presence of disturbances in the model. Unlike gradient-based approaches, the Newton algorithm eliminates the need for the unknown Hessian matrix, allowing for user-assignable convergence rates. The Lyapunov-based switched approach also ensures asymptotic convergence to the optimal set point. Simulation results demonstrate that the proposed approach, combining Newton's method with user-assignable convergence rates and a Lyapunov-based switch, outperforms gradient-based extremum seeking in the hierarchical control framework. [DOI: 10.1115/1.4064088]

Keywords: Newton-based extremum seeking, Lyapunov-based switching, filtered feedback linearization control, hierarchical control framework, control applications, dynamics and control, feedback linearization, intelligent transportation systems, modeling

1 Introduction

In the realm of freeway traffic, congestion frequently occurs at bottleneck locations, where multiple bottlenecks can simultaneously arise in a network during peak rush hours [1]. Many traffic management techniques, encompassing infrastructure-based and vehicle-based strategies, have been developed to optimize traffic flow and enhance road safety [2]. Vehicle-oriented control algorithms focus on designing control systems for individual vehicles, while infrastructure-centric algorithms employ macroscopic models of traffic networks to improve the collective behavior of traffic, including overall traffic flow. The development of traffic controllers for large-scale traffic networks presents notable challenges stemming from the variability in control characteristics and critical parameters among vehicles.

To mitigate these concerns, research efforts have been directed toward developing control approaches that necessitate minimal or no information regarding the dynamics of the traffic network. Examples of such approaches include extremum seeking (ES) control and filtered feedback linearization (FFL) techniques [3].

Filtered feedback linearization is a renowned control technique recognized for its remarkable parameter-stabilizing properties, rendering it a potent approach for realizing local asymptotic stability of the zero dynamics [4]. Compared to the conventional FL approach, the FFL controller demands minimal dynamic model information, namely the dynamic-inversion matrix and the relative degree vector. Moreover, FFL has the advantageous capability of achieving arbitrarily small $\mathcal{L}_\infty$ commands following error, even in the presence of unknown disturbances [5].

In our recent study [6], we employed the FFL approach for the first time in a non-signalized traffic network to achieve the desired density in the target cell. The desired densities were determined based on simulation data, where they were set equal to the critical density of each vehicle class. However, it should be noted that the critical density may not always be the optimal choice due to the intricate dynamics of large-scale traffic networks. Consequently, to address this issue, a hierarchical control framework was introduced in our subsequent publication [7]. Our innovative approach entailed the utilization of gradient-based ES at the upper level, coupled with FFL at the lower level, to mitigate congestion in a traffic network effectively. Specifically, the FFL technique was utilized to modify the communicated velocity to the vehicles,

[1]Paper presented at the 2023 Modeling, Estimation, and Control Conference (MECC 2023), Lake Tahoe, NV, Oct. 2–5. Paper No. MECC2023-162.
[2]Corresponding author.
Manuscript received July 21, 2023; final manuscript received November 2, 2023; published online December 7, 2023. Assoc. Editor: Peter H. Meckl.

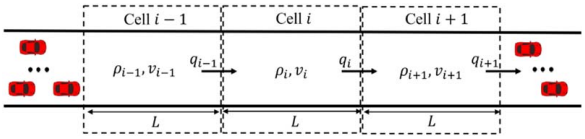

Fig. 1 Discretized traffic network in the METANET model

with the ultimate objective of attaining the target density as determined by the ES. The conventional gradient-based ES control is a model-free optimization approach that focuses on enhancing the steady-state performance of dynamic systems. An ES controller adaptively adjusts the system input to optimize the steady-state output, such as cost or performance, with minimal prior knowledge about the underlying system dynamics [8].

In this study, we enhance the performance of the novel hierarchical control framework by incorporating Lyapunov-based switched Newton extremum seeking (LSNES) at the upper level of the control hierarchy and FFL at the lower level. One of the key distinctions between the Newton algorithm and the gradient algorithm is that the convergence of the former is not solely contingent on the second derivative (Hessian) of the map. In fact, the convergence of the Newton algorithm can be arbitrarily assigned without relying on the properties of the Hessian [9]. This characteristic of the Newton algorithm becomes especially significant in non-model-based algorithms, such as ES, where the Hessian is unknown.

Hence, addressing the limit cycle and achieving asymptotic convergence to the optimal set point is one of the main challenges in the NES. To overcome this challenge, we introduced a Lyapunov-based switched approach that ensures asymptotic convergence to the optimal set point [10]. This ensures stable and robust convergence behavior of the control system, even in the presence of uncertainties. The use of a Lyapunov-based switch provides a rigorous mathematical framework for stability analysis, which enhances the reliability and robustness of the control system. The switched approach allows for adaptability and flexibility in selecting the appropriate control action based on the system's current state, which can be beneficial in complex and dynamic systems such as traffic networks.

Section 2 provides an overview of the traffic dynamics model. Section 3 elaborates on the development of a multi-level control platform for the purpose of realizing desirable traffic dynamics. Section 4 details the simulation results of the hierarchical control framework. Finally, Sec. 5 summarizes the research's key findings, and presents suggestions for future research directions.

2 Dynamic Modeling of Homogeneous Traffic Network

In the discretized traffic network, as depicted in Fig. 1, each cell is denoted as $\mathcal{C}_i$, where $i \in 1, 2, \ldots, n$, and is characterized by three essential parameters: vehicle density (ρi), the average velocity (v_i), and total average flowrate (q_i). In this paper, the METANET model, as proposed by Ref. [11], is adopted to capture the high-level dynamics of the traffic network, utilizing ρ_i and v_i as traffic state variables.

The behavior of $\mathcal{C}_i$ is characterized by

$$\dot{\rho}_i(t) = \frac{1}{\lambda_i L_i}(q_{i-1}(t) - q_i(t) + d_i(t)) \tag{1a}$$

$$\dot{v}_i(t) = \frac{1}{\tau_i}\Big(U_i(t) - v_i(t)\Big) + \frac{1}{L_i}\left[v_i(t)\Big(v_{i-1}(t) - v_i(t)\Big) - \frac{\varepsilon_i}{\tau_i}\frac{\rho_{i+1}(t) - \rho_i(t)}{\rho_i(t) + \kappa_i}\right] \tag{1b}$$

$$q_i(t) = \rho_i(t) v_i(t) \tag{1c}$$

λ_i denotes the lane count, while L_i represents the length of each individual cell (for simplicity, we assumed $L_i = L$). $d_i(t)$ is uncontrolled flow (disturbance), including the ramp flows, and $U_i(t) = (1 - \beta_i(t))\mathcal{V}_i(t)$ is regarded as the recommended speed within each cell, where $\mathcal{V}_i(t) = v_f \exp\left[\frac{-1}{a_{m,i}}\left(\frac{\rho_i(t)}{\rho_{cr}}\right)^{a_{m,i}}\right]$ depicts the relationship between velocity and density in a steady-state condition [12]. ρ_{cr} is the critical density, and v_f is the free-flow. Also, ε_i, κ_i, τ_i, and $a_{m,i}$ are METANET model parameters that are dependent on the states of each cell. We introduce the control command $\beta_i(t)$, where $0 \le \beta_i(t) \le 1$, as a means to adjust the suggested (recommended) velocity of each cell. In the absence of any control, denoted by $\beta_i(t) = 0$, the system operates without intervention, and its macroscopic dynamics conform to the steady-state velocity-density behavior. Conversely, when $\beta_i(t) = 1$, it indicates that the controller recommends the vehicles come to a complete stop as per the prescribed control action.

Traffic dynamics in Eqs. (1*a*)–(1*b*) can be mathematically expressed as

$$\dot{x}(t) = f(x(t)) + B(x(t))u(t) + \mathcal{D}(t) \tag{2a}$$

$$y(t) = G(x(t)) \tag{2b}$$

where $t \ge 0$; $y(t) = [\rho_s(t), \cdots, \rho_m(t)]^T \in \mathbb{R}^{m-s+1}$ where $s \ge 2$ and $m \le n$ is the output vector, $x(t) = [\rho_1(t) \ \cdots \ \rho_n(t) \ v_1(t) \ \cdots \ v_n(t)]^T \in \mathbb{R}^{2n}$ is the state vector, $u(t) = [\beta_{s-1}(t) \ \cdots \ \beta_m(t)]^T \in \mathbb{R}^{m-s+2}$ is the control input vector, $f(x(t)) = [\dot{\rho}_1(t) \ \cdots \ \dot{\rho}_n(t) \ \hat{v}_1(t) \ \cdots \ \hat{v}_n(t)]^T \in \mathbb{R}^{2n}$ where $\hat{v}_i(t) = \frac{1}{\tau}\Big(\mathcal{V}_i(t) - v_i(t)\Big) + \frac{v_i}{L}(t)\Big(v_{i-1}(t) - v_i(t)\Big) - \frac{\varepsilon}{L\tau}\frac{\rho_{i+1}(t) - \rho_i(t)}{\rho_i(t) + \kappa}$, $B(x(t)) = \Big[[0]_{(m-s+2\times n)}\,[0]_{(m-s+2\times s-2)}\,[\hat{B}]_{(m-s+2\times m-s+2)}\,[0]_{(m-s+2\times n-m)}\Big]^T$ where $\hat{B} = -\frac{1}{\tau}\text{diag}\{\mathcal{V}_{s-1}, \ldots, \mathcal{V}_m\}$, and $\mathcal{D}(t) = [\mathcal{D}_1(t) \cdots \mathcal{D}_{2n}(t)]^T \in \mathbb{R}^{2n}$ is the disturbance. The dimensionality of the input vector $u(t)$ is greater than that of the output vector $y(t)$ due to the constraints imposed on the control command ($0 \le \beta(t) \le 1$). Efficient regulation of vehicle density in cell $\mathcal{C}_i$ requires two control inputs for recommended velocities in $\mathcal{C}_{i-1}$ (upstream cell) and $\mathcal{C}_i$ (target cell). These commands can be adjusted to modify inflow and outflow, enabling dynamic density control within $\mathcal{C}_i$ based on the controllability matrix from Ref. [13].

3 Hierarchical Control Framework Design

This section is dedicated to the design of a distributed multi-level macroscopic traffic control framework (LSNES-FFL) with the objective of enhancing the mobility of congested traffic. The primary aims of this control strategy are to (i) optimize the performance of the overall system by mitigating congestion, (ii) proactively prevent the retrograde propagation of congestion, and (iii) consistently maintain the desired density set-point values.

3.1 Lower-Level Controller: Filtered Feedback Linearization. Within the envisioned hierarchical traffic management framework design, the lower-level utilizes an FFL approach to dynamically modify the communicated recommended velocities for the vehicles. The objective is to attain the desired density values as determined by the infrastructure or the upper-level controller. The utilization of the FFL controller in this framework depends on the understanding of the dynamic-inversion matrix and relative degree, as explained in Ref. [5]. More specifically, for a given cell $\mathcal{C}_i$, the FFL design assumes a relative degree ($\bar{r}$) of 2 for u_i and u_{i-1} with respect to y_i. Now consider the following assumptions which are necessary for FFL control design:

ASSUMPTION 1. *The input of the reference model, denoted as $\rho^d(t)$, is assumed to be bounded and possesses differentiability properties up to $\bar{r}$th order.*

ASSUMPTION 2. *The disturbance term $\mathcal{D}(t)$ is assumed to exhibit continuity and differentiability up to the $(\bar{r} - 1)$th order.*

The error term is $E(t) = y(t) - y_m(t)$. The primary goal is to design u that achieves asymptotic stabilization of the closed-loop system

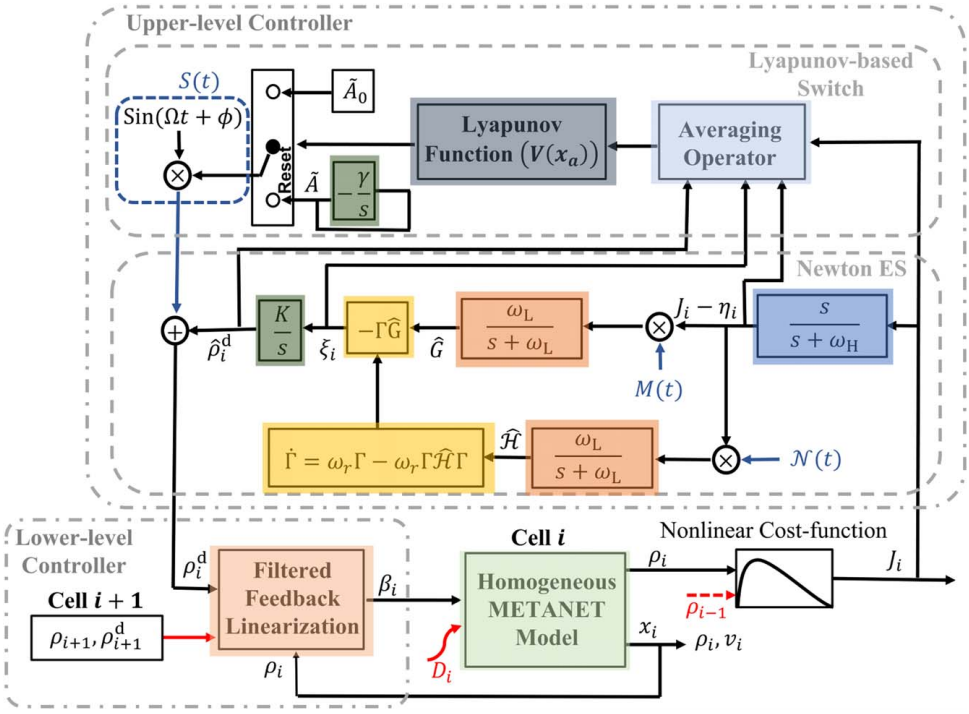

Fig. 2 Comprehensive schematic of the control framework design for $\mathcal{C}_i$ consisting of the Newton ES, Lyapunov-based switch, FFL, and METANET model

while simultaneously minimizing the square root of the average power of the density error $\mathcal{P}_E = \left[\frac{1}{t_1-t_0}\int_{t_0}^{t_1} E^{\text{T}}(\tau)E(\tau)\,\text{d}\tau\right]^{\frac{1}{2}}$ to arbitrarily small levels. In pursuit of this objective, the desired FL control input is expressed as follows [4]:

$$u^{\text{d}}(x,\Phi_r,\Phi_{\mathcal{D}}) = -M_{\text{u}}^{-\dagger}(M_{\text{u}}M_{\text{u}}^{-\dagger})^{-1}(\nu(x,\Phi_r,\Phi_{\mathcal{D}})+\Psi(x,\Phi_{\mathcal{D}})) \quad (3)$$

where $\Phi_r=[\rho^{\text{d}}\ \dot{\rho}^{\text{d}}\ \ddot{\rho}^{\text{d}}]^{\text{T}}$, $\Phi_{\mathcal{D}}=[\mathcal{D}\ \dot{\mathcal{D}}]^{\text{T}}\Psi(x,\Phi_{\mathcal{D}})=C\frac{\partial f}{\partial x}(f(x)+\mathcal{D})$, $+C\dot{\mathcal{D}}$. Furthermore, $\nu(x,\Phi_r,\Phi_{\mathcal{D}})=\ddot{\rho}^{\text{d}}+\zeta_1\dot{\rho}^{\text{d}}+\zeta_0\rho^{\text{d}}-\alpha_1\dot{y}_{\text{m}}-\alpha_0 y_{\text{m}}$ where y_{m} is the local reference model and α_0, α_1, ζ_0, ζ_1 are constants. $M_{\text{u}}=C\frac{\partial f(x(t))}{\partial x}B(x(t))$ and $M_{\text{u}}^{-\dagger}$ is the pseudo inverse of it. The ideal control input u^{d} is not feasible for implementation due to its dependency on the knowledge of the underlying dynamic $f(x(t))$, measurement of the full state $x(t)$, and unknown disturbances $\mathcal{D}(t)$. To tackle this challenge, we make an assumption that the desired input u^{d} gained from FL possesses sufficient smoothness, as represented as follows:

ASSUMPTION 3. *For $i\in N$, $\frac{\partial}{\partial x}[u_i^{\text{d}}(x,\Phi_{\mathcal{D}},\Phi_r)]$ and $\frac{\partial}{\partial\Phi_{\mathcal{D}}}[u_i^{\text{d}}(x,\Phi_{\mathcal{D}},\Phi_r)]$ exist and are continuous.*

The control input u for implementation is derived by filtering the desired control input u^{d} using the designed filter. Specifically,

$$[\mathbf{p}\bar{\varrho}_z(\mathbf{p})I+\varrho_z(0)M_{\text{u}}'M_{\text{u}}]u=\varrho_z(0)M_{\text{u}}'M_{\text{u}}u^{\text{d}} \quad (4)$$

where M_{u}' is the transpose of M_{u}, $\mathbf{p}=d/dt$, $\varrho_z(s)$ is a polynomial with a degree $q\geq 2$ which must satisfy specific conditions as outlined in Ref. [4]. Therefore, the FFL control input is

$$\mathbf{p}\bar{\varrho}_z(\mathbf{p})u=\varrho_z(0)M_{\text{u}}'[\ddot{\rho}^{\text{d}}+\zeta_1\dot{\rho}^{\text{d}}+\zeta_0\rho^{\text{d}}-\ddot{y}-\alpha_1\dot{y}-\alpha_0 y] \quad (5)$$

Mathematically, the controllers (3) and (5) are equivalent. However, FFL control input in Eq. (5) does not require $\Psi(x,\Phi_{\mathcal{D}})$, $\mathcal{D}$, or $\dot{\mathcal{D}}$, unlike the FL control input in Eq. (3).

PROPOSITION 1. *Under the Assumptions 1–3, the minimum phase system, as described by Eqs. (2)–(5), demonstrates asymptotic stability when the filter polynomial ϱ_z possesses a sufficiently large z value.*

Proof. The proof can be found in Refs. [4,5]. ∎

Remark 1. Choosing a suitably large value of z in the filter polynomial ϱ_z allows for the performance index $\mathcal{P}_E$ to be minimized to arbitrarily small levels.

3.2 Upper-Level Controller: LSNES. In Ref. [7], we implemented a gradient-based ES at the upper level of the hierarchical control framework. In this study, in order to achieve faster convergence and improve the performance of the hierarchical control framework, an LSNES is employed at the upper level to compute the optimal density of target cells, denoted as ρ_i^{d}. The results obtained from our research in Ref. [7] reveal two significant insights: (i) the ES algorithm, which relies on gradient-based optimization, exhibits local convergence and (ii) the speed of convergence is impacted by the Hessian matrix denoted as $\mathcal{H}$ which is unknown. One noteworthy feature of the Newton-based algorithm is its capacity to reduce dependence on the unknown $\mathcal{H}$ when determining the rate of convergence. Furthermore, several existing methods often tend to converge to a limit cycle around the desired state, instead of achieving precise convergence to it. Therefore, a significant challenge in utilizing the NES is to eliminate the limit cycle behavior and achieve asymptotic convergence to the optimal set point. To address this challenge, we incorporated a Lyapunov-based switch into the NES approach, which enables asymptotic convergence to the optimal set point.

3.2.1 Newton Extremum Seeking Algorithm. The Newton-based algorithm encompasses two critical elements: $\mathcal{N}(t)$, which represents the perturbation matrix and gives us an approximation of the Hessian matrix, and the Riccati equation, which yields an estimation of the inverse of $\mathcal{H}$, even in scenarios where the estimation of the $\mathcal{H}$ is singular. In Ref. [9], it has been shown that by carefully choosing an appropriate matrix denoted as $\mathcal{N}(t)$ and calculating the average value of $\hat{\mathcal{H}}=\mathcal{N}(t)y$ over a period denoted as π, which is associated with the perturbation frequency Ω_i, an estimation of the Hessian matrix can be obtained.

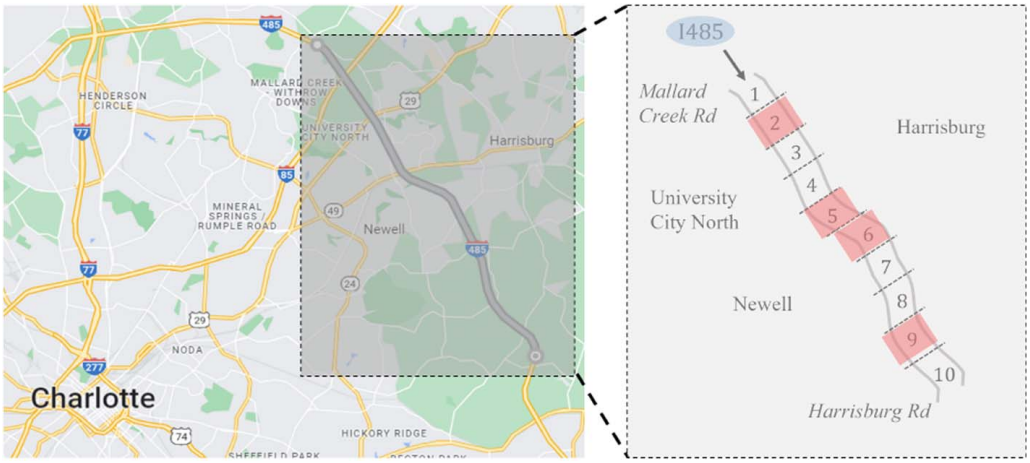

Fig. 3 I-485, Charlotte, NC (between Mallard Creek and Harrisburg Road). Congested cells are highlighted.

Subsequently, we shall establish the definition of the cost function and formulate the optimization problem in the following manner:

$$\max_{\rho_i} \; J_i(t) = \bar{w}_{i,1}(t)\mathcal{Q}_i^2(t) - \bar{w}_{i,2}(t)[\mathcal{Q}_i(t) - \mathcal{Q}_{i-1}(t)]^2 \tag{6}$$

The weights denoted by $w_{i,1}(t)$ and $w_{i,2}(t)$ in the cost function, along with the term $\mathcal{Q}_i(t) = \rho_i(t)\mathcal{V}_i(t)$. It should be noted that $\mathcal{Q}_i(t)$ is subject to the dynamics described in Eqs. (2) and (5), resulting in the following expression for the lower-level dynamics:

$$\dot{X}_{\mathrm{LL}} = \mathcal{F}_{\mathrm{LL}}\left(X_{\mathrm{LL}}, \mathcal{G}(X_{\mathrm{LL}}, \rho^{\mathrm{d}})\right) \tag{7}$$

where $X_{\mathrm{LL}} = [x \; u \; \dot{u} \; \ldots \; u^{(b-1)}]$.

To tackle the optimization problem presented in Eq. (6), we propose an LSNES controller. The LSNES controller, as depicted in Fig. 2, employs sinusoidal signals defined as $S(t) = \tilde{A}_i(t)\sin(\Omega_i.t + \phi)$ and $M(t) = \dfrac{2}{\tilde{A}_i(t)}\sin(\Omega_i.t + \phi)$. As a result, a feasible choice for $\mathcal{N}(t)$, which satisfies all necessary constraints, can be obtained as proposed in Ref. [9].

$$\mathcal{N}(t) = \frac{16}{\tilde{A}(t)^2}\left(\sin^2(\Omega_i.t) - \frac{1}{2}\right) \tag{8}$$

The computation of the inverse of the Hessian matrix, denoted as Γ, can pose difficulties in cases where the matrix $\hat{\mathcal{H}}$ is in close proximity to singularity. To tackle this challenge, we employ a dynamic estimator that calculates the inverse of $\hat{\mathcal{H}}$ utilizing a Riccati equation, as exemplified as follows:

$$\dot{\Gamma} = \omega_r - \omega_r \Gamma \hat{\mathcal{H}} \Gamma \tag{9}$$

where ω_r is a positive value and the equilibria of the Riccati in Eq. (9) is $\Gamma^* = 0$ (unstable) and $\Gamma = \hat{\mathcal{H}}^{-1}$ (exponentially stable), provided $\hat{\mathcal{H}}$ to a constant. To ensure that the underlying dynamics exhibit a static nonlinearity when viewed from the NES loop perspective, it is crucial to select a perturbation frequency Ω_i that is sufficiently small, as discussed in Ref. [8]. Specifically, we consider $\Omega_i = \mathcal{O}(\omega)$, where $\omega_{\mathrm{i,H}} = \mathcal{O}(\Delta\omega)$ and $\omega_{\mathrm{i,L}} = \mathcal{O}(\Delta\omega)$, with $\mathcal{O}$ denoting statistical order, and ω and Δ representing small positive constants.

Remark 2. It is noteworthy that the convergence time of the NES to the desired density is substantially slower in comparison to the response time of the inner loop. Consequently, it is justifiable to assume that the density reference remains relatively constant in contrast to the dynamics of the inner loop.

In order to uphold the stability of the NES controller, a series of assumptions must be satisfied, as posited in the literature [9].

ASSUMPTION 4. *Smooth mapping function $\ell : \mathbb{R}^n \to \mathbb{R}^{m-s+1}$ is assumed, such that the $\mathcal{F}_{\mathrm{LL}}\left(X_{\mathrm{LL}}, \mathcal{G}(X_{\mathrm{LL}}, \rho^{\mathrm{d}})\right) = 0$ holds if and only if $X_{\mathrm{LL}} = \ell(\rho^{\mathrm{d}})$.*

ASSUMPTION 5. *The equilibrium $x = \ell(\rho^d)$ of the system $\dot{X}_{\mathrm{LL}} = \mathcal{F}_{\mathrm{LL}}\left(X_{\mathrm{LL}}, \mathcal{G}(X_{\mathrm{LL}}, \rho^{\mathrm{d}})\right)$ is locally exponentially stable, with uniform stability across $\rho^{\mathrm{d}} \in \mathbb{R}^{m-s+1}$.*

ASSUMPTION 6. *The existence of a $\rho^{\mathrm{d}} \in \mathbb{R}^{m-s+1}$ is assumed, such that $\dfrac{\partial}{\partial\rho}J(\rho^{\mathrm{d}}) = 0$ and $\dfrac{\partial^2}{\partial^2\rho}J(\rho^{\mathrm{d}}) < 0$.*

Assumptions 4 and 5 are supported by the assured asymptotic stability of the lower-level dynamics by the FFL controller, as stated in Proposition 1. Furthermore, Assumption 6 is met due to the quadratic nature of the cost function in Eq. (6), which is derived from the macroscopic fundamental diagram (MFD).

The proposition presented below provides a summary of the stability and convergence characteristics of the upper-level NES controller:

PROPOSITION 2. *Under Assumptions 4–6, the closed-loop feedback system shown in Fig. 2 achieves exponential convergence for any solution starting from a neighborhood of the point $(x, \rho^{\mathrm{d}}, \xi, \eta) = \left(\ell(\rho^{\mathrm{d}}), \rho^{\mathrm{d}}, 0, J(\rho^{\mathrm{d}})\right)$. This holds for a given $\omega \in (0, \bar{\omega})$, where $\bar{\omega}$, $\bar{\Delta}$, and $\bar{A}$ are positive constants. Furthermore, the output $y(t)$ also converges to an $\mathcal{O}(\omega + \Delta + |\tilde{A}|)$-neighborhood of $J(\rho^d)$, for any $\Delta \in (0, \bar{\Delta})$ and $|\tilde{A}| \in (0, \bar{A})$. It's worth noting that Remark 2 is applicable in this context.*

Proof. The proof can be found in Ref. [9]. ∎

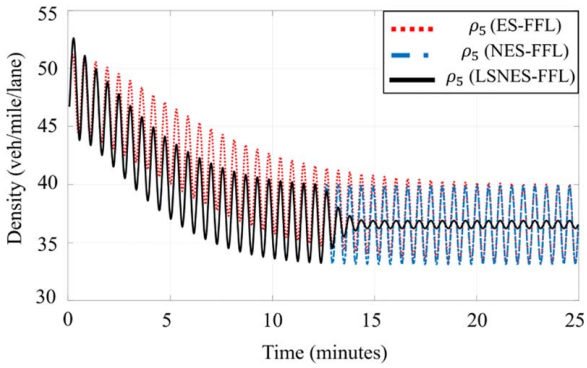

Fig. 4 Target cell 5 density changes using ES-FFL (dotted line), NES-FFL (dash-dotted line), and LSNES (solid line). The Newton-based ES has 48% faster convergence rate in comparison to gradient-based ES.

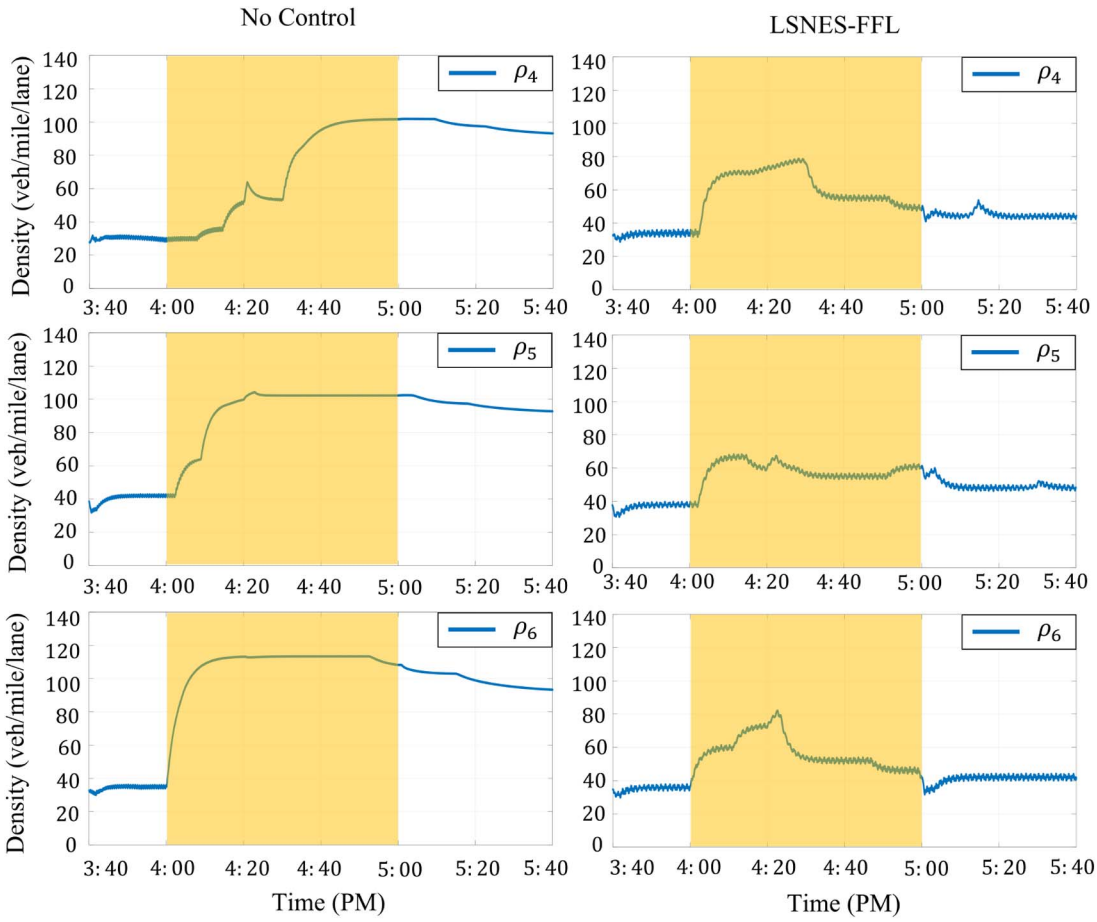

Fig. 5 Density behavior for cells 4, 5, and 6 in both no active controller and active LSNES controller

3.2.2 Lyapunov-Based Switch. To address the potential loss in optimality that may arise due to continuous sinusoidal perturbations around the optimal point, we propose a switched control scheme to be added to the NES structure. The proposed switched control scheme involves reducing the amplitude of perturbations after convergence, specifically within a neighborhood around the desired state. The switch proposed by Ref. [10] is determined by utilizing a Lyapunov function that is based on an averaged model of the ES feedback system. This Lyapunov function is designed to approximate the proximity to the desired state, and based on this estimate, the switch is activated to reduce the perturbation size.

The Lyapunov function utilized in the LSNES is a function of an averaged state variable, which is obtained by taking the average over one oscillation period. This Lyapunov function is given by

$$\tilde{x}_a = \frac{\Omega}{2\pi}\int_{t-\frac{2\pi}{\Omega}}^{t} \tilde{x}(\tau)\,\mathrm{d}(\tau) \tag{10}$$

where $\tilde{x} = [\tilde{\rho}^{\mathrm{d}}, \xi, \tilde{\eta}]^{\mathrm{T}}$ as shown in Fig. 2. The switching mechanism illustrated in Fig. 2 utilizes a quadratic Lyapunov function denoted as $V(\tilde{x}_a)$, which serves as a metric for gauging the closeness of the averaged values (computed over one NES period) of ρ^{d} and η to their estimated desired values.

$$V(\tilde{x}_a) = \frac{1}{2}\tilde{x}^{\mathrm{T}}\bar{J}\tilde{x} \tag{11}$$

The construction of V involves solving the following Lyapunov equation for $\bar{J}$ considering $Q = Q^{\mathrm{T}} > 0$:

$$\bar{J}J_{\mathrm{a}} + J_{\mathrm{a}}^{\mathrm{T}}\bar{P} = -Q \tag{12}$$

where the Jacobian matrix J_{a} is utilized to approximate the system dynamics near the equilibrium [10] as follows:

$$J_{\mathrm{a}} = \begin{bmatrix} 0 & \hat{K}' & 0 \\ \omega_\ell' h''(0) A_0 & -\omega_\ell' & 0 \\ \omega_{\mathrm{h}}' h'(0) & 0 & -\omega_{\mathrm{h}}' \end{bmatrix} \tag{13}$$

where $\hat{K} = \dfrac{K}{\Omega}$, $\omega_\ell' = \dfrac{\omega_{\mathrm{L}}}{\Omega}$, $\omega_{\mathrm{h}}' = \dfrac{\omega_{\mathrm{H}}}{\Omega}$, $h'(0) = J'(\rho^{\mathrm{d}})$, and $h''(0) = J''(\rho^{\mathrm{d}}) < 0$. When the value of $V(\tilde{x}_{\mathrm{a}})$ is small enough, the perturbation signal, $A(t)$, will decay in size. However, if $V(\tilde{x}_{\mathrm{a}})$ is not sufficiently small, the perturbation signal will remain at its full size. The following relationship dictates how the size of $A(t)$ changes over time.

$$A(t) = \begin{cases} A_0 & \text{if } V(\tilde{x}_{\mathrm{a}}) > \varepsilon \\ -\gamma\displaystyle\int_{t_{sw}}^{t} A(\tau)\,\mathrm{d}(\tau) & \text{if } V(\tilde{x}_{\mathrm{a}}) \le \varepsilon \end{cases} \tag{14}$$

where t_{sw} is the switching time and γ determines the rate at which the perturbation amplitude shrinks in the proposed control scheme.

Remark 3. In scenarios where the optimal density (ρ^{d}) and its corresponding cost function value ($J(\rho^{\mathrm{d}})$) are not known a priori, an estimation procedure is employed to approximate these values, as well as h' and h'', for use in Eq. (12). This estimation process involves numerically differentiating J and J' based on the current and previous values to estimate h' and h'' at the current density. Subsequently, extrapolation is utilized to estimate ρ^{d} using the values of J' and J'' at the current density. Previous studies [10] have demonstrated the algorithm's robustness to estimation errors.

4 Simulation Results and Discussion

Here, we evaluate the effectiveness of the novel hierarchical control framework design. The schematic of the section used in the conducted case studies is depicted in Fig. 3. The freeway section under consideration has an approximate length of 10 miles, a speed limit of 70 mph, and consists of four lanes. The network is discretized into 10 cells, as illustrated in Fig. 3.

The METANET model parameters are selected to be $\varepsilon = 38\,\text{mile}^2/\text{h}$, $\kappa = 18$ veh/mile.h, $\tau = 2.5$ s, $\lambda = 4$, and $a_m = 3.8$. Furthermore, $\rho_c = 31$ veh/mile.lane, the jam density is $\rho_J = 162$ veh/mile.lane, $v_f = 70$ mph, and $q_0 = 2200$ veh/h. Model parameters for the target cells (2, 5, 6, and 9) are obtained from PTV-VISSIM simulations using traffic flow data from I-485 N of Exit 28 on Tuesday, Dec. 22, 2020, during the peak time period of 4–5 p.m. Measured states from the simulations are compared with the METANET model to determine the parameters. Finally, we have $w_{i,1} = w_{i,2} = 1$, $A_0 = 5$, $\varepsilon = 1$ $\Omega_i = 0.01\pi$ rad/s, $\omega_{i,L} = 0.1\Omega_i$, $\omega_{i,H} = 0.2\Omega_i$, $K_i = 1.35$, and $z = 1$.

In Ref. [7], we compared our designed hierarchical control framework (ES-FFL) with a common large-scale traffic control algorithm, the PID mainstream traffic flow control (PID-MTFC) approach. It was shown that the ES-FFL has a better performance in terms of congestion reduction and preventing congestion back-propagation with respect to the PID-MTFC and also has a faster convergence rate. In this section, we begin by comparing the performance of the designed LSNES-FFL control with that of the ES-FFL control to show the effectiveness of the improved upper-level controller in large-scale traffic control. The quadratic map in Eq. (6) is used to compare the gradient-based and Newton-based ES methods. All parameters are kept the same except for the gain matrix to ensure a fair comparison. For the Newton-based method, the convergence rate is governed by $-K_N\Gamma(t)\mathcal{H}$, while the gradient-based scheme depends on the eigenvalues of $K_G\mathcal{H}$. Therefore, to ensure fairness, K_G is selected as $-K_N\Gamma_0$.

Here, the target cell 5 is considered, and different controllers (ES-FFL, NES-FFL, LSNES-FFL) in three different simulation runs are active to control the traffic, reduce the congestion, and prevent congestion back-propagation. As shown in Fig. 4, the Newton ES has a faster convergence to the desired density with respect to the gradient-based ES approach (48% improvement). By adding the Lyapunov-based switch, the perturbation size is reduced after entering the neighborhood around the desired density to control the traffic better and increase its robustness.

Subsequently, we validate the effectiveness of the LSNES-FFL controller in alleviating congestion and mitigating back-propagating congestion through a numerical example. The case study entails a comparison of two scenarios: the first scenario, where no active infrastructure controller is present in the traffic network, and the second scenario, where a local LSNES-FFL controller is deployed for target cells in the traffic network. Specifically, target cells 2, 5, 6, and 9 are identified as being prone to heavy congestion due to an unknown downstream bottleneck. In Fig. 5, the density profiles of cells 5 and 6, as well as upstream cell 4, are displayed for both the "LSNES-FFL" and "No-Control" scenarios. It is evident that in the absence of control, congestion begins to back-propagate, resulting in more severe congestion as density increases. However, by activating the local "LSNES-FFL" controller, which estimates and tracks optimal densities, the target cells effectively avoid jam conditions.

5 Conclusions and Future Work

The primary focus of this paper is to enhance the performance of a hierarchical control framework for large-scale traffic networks. We designed and implemented LSNES at the upper level of the hierarchy to feed the optimal density of congested cells to the lower-level controller (FFL). The Newton algorithm eliminates the need for the unknown Hessian matrix, allowing for user-assignable convergence rates. Additionally, the Lyapunov-based switched approach ensures asymptotic convergence to the optimal set point. The simulation results showed that the LSNES-FFL has a 48% faster convergence rate with respect to the conventional ES-FFL method. In the future, to capture the traffic system's realistic nature and have a high-fidelity model, the uncertainties associated with the unmodeled dynamics, which can intrinsically be state-dependent, will be learned using online data-driven modeling approaches.

Acknowledgment

This material is based upon work supported by the National Science Foundation (Grant No. 2130704) and the North Carolina Department of Transportation.

Conflict of Interest

There are no conflicts of interest.

Data Availability Statement

The datasets generated and supporting the findings of this article are obtainable from the corresponding author upon reasonable request.

References

[1] Markantonakis, V., Skoufoulas, D. I., Papamichail, I., and Papageorgiou, M., 2019, "Integrated Traffic Control for Freeways Using Variable Speed Limits and Lane Change Control Actions," Transp. Res. Record, **2673**(9), pp. 602–613.

[2] Mehr, N., and Horowitz, R., 2019, "How Will the Presence of Autonomous Vehicles Affect the Equilibrium State of Traffic Networks?" IEEE Trans. Contr. Netw. Syst., **7**(1), pp. 96–105.

[3] Li, D., and Hou, Z., 2020, "Perimeter Control of Urban Traffic Networks Based on Model-Free Adaptive Control," IEEE Trans. Intell. Transp. Syst., **22**(10), pp. 6460–6472.

[4] Hoagg, J. B., and Seigler, T. M., 2013, "Filtered-Dynamic-Inversion Control for Unknown Minimum-Phase Systems With Unknown-and-Unmeasured Disturbances," Int. J. Contr., **86**(3), pp. 449–468.

[5] Ghasemi, A. H., 2017, "Slewing and Vibration Control of a Single-Link Flexible Manipulator Using Filtered Feedback Linearization," J. Intell. Mater. Syst. Struct., **28**(20), pp. 2887–2895.

[6] Shahri, P. K., and Ghasemi, A. H., 2022, "Heterogeneous Traffic Management Using METANET Model With Filtered Feedback Linearization Control Approach," Technical Report, SAE Technical Paper.

[7] Shahri, P. K., HomChaudhuri, B., Pulugurtha, S. S., Mesbah, A., and Ghasemi, A. H., 2022, "Traffic Congestion Control Using Distributed Extremum Seeking and Filtered Feedback Linearization Control Approaches," IEEE Control Syst. Lett., **7**, pp. 1003–1008.

[8] Krstić, M., and Wang, H., 2000, "Stability of Extremum Seeking Feedback for General Nonlinear Dynamic Systems," Automatica, **36**(4), pp. 595–601.

[9] Ghaffari, A., Krstić, M., and Nešić, D., 2012, "Multivariable Newton-Based Extremum Seeking," Automatica, **48**(8), pp. 1759–1767.

[10] Bafandeh, A., and Vermillion, C., 2016, "Altitude Optimization of Airborne Wind Energy Systems Via Switched Extremum Seeking–Design, Analysis, and Economic Assessment," IEEE Trans. Control Syst. Technol., **25**(6), pp. 2022–2033.

[11] Wang, Y., Yu, X., Guo, J., Papamichail, I., Papageorgiou, M., Zhang, L., Hu, S., Li, Y., and Sun, J., 2022, "Macroscopic Traffic Flow Modelling of Large-Scale Freeway Networks With Field Data Verification: State-of-the-Art Review, Benchmarking Framework, and Case Studies Using Metanet," Transp. Res. Part C: Emerg. Technol., **145**, p. 103904.

[12] Daganzo, C. F., and Geroliminis, N., 2008, "An Analytical Approximation for the Macroscopic Fundamental Diagram of Urban Traffic," Transp. Res. Part B: Methodol., **42**(9), pp. 771–781.

[13] Muñoz, L., Sun, X., Horowitz, R., and Alvarez, L., 2003, "Traffic Density Estimation With the Cell Transmission Model," Proceedings of the 2003 American Control Conference, Denver, CO, June 4–6, Vol. 5, IEEE, pp. 3750–3755.